Only 3 Spatial Patterns of Tidal Heating. Mikael Beuthe, Attilio Rivoldini and Véronique Dehant, Royal Observatory of Belgium, Brussels, Belgium, (mbeuthe@oma.be).

Introduction:

The power dissipated by tidal deformations within a body varies with latitude and longitude and depth, as Kaula already observed in 1964 [1]. While the total dissipated power is the quantity of utmost interest for the orbital dynamics and global thermal state, spatial variations in the dissipation rate are also of great interest in planetology. For instance they have been used in order to predict the distribution of volcanism on Io [2, 3], the thickness variations of the ice layer on icy satellites [4], or the tectonic patterns on Mercury [5]. A point of special interest is the possibility of using surface heat flux patterns in order to constrain the internal structure [6].

At a given point within the planet, the power dissipated by tides per unit volume is

$$P(t) = \sum_{i,j} \sigma_{ij}(t) \, \frac{d}{dt} \epsilon_{ij}(t) \,, \qquad (1)$$

where $\sigma_{ij}(t)$ are the stresses and $\epsilon_{ij}(t)$ are the strains.

The standard procedure [7, 2, 8] for the computation of the power consists in:

1. averaging the power over time after having expanded the stress and strain in Fourier series,
2. assuming a type of rheology so that the stress can be expressed in terms of the strain,
3. modeling the body as spherically concentric layers (physically relevant parameters are the density, shear modulus μ, compressibility and viscosity η),
4. solving the equations for the deformation of the body, so that the strain can be computed at every point (r, θ, ϕ) in terms of the external tidal potential and the six radial functions $y_i(r)$ describing the response of the body [9],
5. computing the power at every point by summing over all terms in Eq. (1).

We assume here that the tides are of degree 2, operate at only one angular frequency ω and that the rheology is of the Maxwell type with non-dissipative compressibility. If these assumptions are modified, there is no difficulty in adapting the formulas given below.

Factorization in radial and angular parts:

Until now, the power had to be computed at every point since first and second derivatives of the tidal potential with respect to θ and ϕ appear in various combinations. We know however that the final result is a scalar under rotations, which implies that the derivatives should combine into scalars. Tensor calculus actually allows us to write the dissipated power in terms of three scalar fields:

$$|\Phi|^2, \; \Delta|\Phi|^2, \; \Delta^2|\Phi|^2 \,, \qquad (2)$$

where Δ is the spherical Laplacian with eigenvalues $-\ell(\ell+1)$ (ℓ is the harmonic degree) and Φ is the positive-frequency coefficient of the Fourier-expanded tidal potential. Since Φ is only of degree 2, $|\Phi|^2$ can be expanded in spherical harmonics with $\ell = 0$, 2, or 4 so that $\Delta|\Phi|^2$ and $\Delta^2|\Phi|^2$ can be analytically computed. The angular functions are multiplied by real radial functions that depend on the internal functions $y_i(r)$.

Though very simple, the basis (2) is not convenient for the prediction of spatial patterns because of compensations between the three terms. We thus choose to group the terms differently so that the multiplying radial functions have very different magnitudes in very different interior models. The time-averaged power becomes

$$\bar{P} = \bar{P}_0 + \frac{2\omega}{r^2} \, \mathrm{Im}(\mu) \, \left(f_A \Psi_A + f_B \, \Psi_B + f_C \, \Psi_C \right) \,, \qquad (3)$$

where $\bar{P}_0$ is a constant (see below). Let $\overline{|\Phi|^2}$ be the mean of $|\Phi|^2$. The angular functions are

$$\begin{aligned} \Psi_A &= |\Phi|^2 - \overline{|\Phi|^2} \,, \\ \Psi_B &= (\Delta + 12) \, \Psi_A \,, \\ \Psi_C &= \left(\Delta^2 + 22\Delta + 48\right) \Psi_A \,. \end{aligned} \qquad (4)$$

The radial functions are

$$\begin{aligned} f_A &= 2|ry_1'|^2 + |2y_1 - 6y_3|^2 - \frac{2}{3}|ry_1' + 2y_1 - 6y_3|^2 \\ f_B &= \frac{|ry_4|^2}{2|\mu|^2} \,, \\ f_C &= \frac{|y_3|^2}{2} \,, \end{aligned} \qquad (5)$$

where y_1' is the derivative of y_1 with respect to r. If the body is incompressible, f_A is equal to $12|y_1 - 3y_3|^2$.

In Eq. (3), $\bar{P}_0$ is the spatially uniform part of the time-averaged potential:

$$\bar{P}_0 = \frac{2\omega}{r^2} \, \mathrm{Im}(\mu) \, H_\mu \, \overline{|\Phi|^2} \,. \qquad (6)$$

The radial function H_μ depends on the y_i and coincides with the sensitivity parameter H_μ obtained in [8] with variational methods. The classical formula for the total power dissipated within a synchronous satellite [2] is obtained by integrating $\bar{P}_0$ over the volume. The integral of $\mathrm{Im}(\mu) H_\mu$ can be related to $\mathrm{Im}(k_2)$ with Eq. (35) of [8]. The angular functions $\Psi_{A,B,C}$ do not contribute to the volume-integrated power since they have zero mean.

Spatial patterns:

At any depth, the dissipated power is described by a linear combination of the angular functions $\Psi_{A,B,C}$. In applications, one often assumes radial transport of the dissipated power to the surface, in which case the surface heat flux is given by $\int dr(r/R)^2\bar{P}$. The spatial variations of the surface heat flux are then given by the angular functions $\Psi_{A,B,C}$ with weights obtained by integrating the radial functions $f_{A,B,C}$. Therefore the pattern of the surface heat flux is characterized by three numbers.

The three spatial patterns $\Psi_{A,B,C}$ are illustrated in Fig. 1 for a body in synchronous rotation. Patterns A and B have a significant component of degree 4 whereas Pattern C has nearly none. Though the true spatial pattern is a superposition of the three patterns, one pattern often dominates because of the very different dependences of the functions $f_{A,B,C}$ on the y_i.

As a first example, we have recomputed the two models proposed for Io in [2, 3]. Dissipation mainly occurs in the mantle for Model A and in the asthenosphere for Model B, leading to Pattern C in the former case and Pattern B in the latter (see Figs. 8 and 10 in [2]). The weights of the different patterns are listed in Table 1.

Model	q_A	q_B	q_C
A	0.05	0.09	0.41
B	0.001	0.39	0.0002

Table 1: Heat flux at the surface of Io: weights of Patterns (A,B,C). The heat flux is expressed as $q = q_0(1+q_A\hat{\Psi}_A+q_B\hat{\Psi}_B+q_C\hat{\Psi}_C)$. The ''hat' on the angular functions means that they are normalized by their RMS. For Model A, $\mu=10^{10}$ Pa and $\eta=10^{15}$ Pa.s in the mantle. For Model B, $\mu=10^7$ Pa and $\eta=10^{10}$ Pa.s in the asthenosphere. Values of other parameters are given in [2].

As a second example, we compare Patterns (A,B,C) with the patterns computed in [8] for a large icy satellite. Pattern C represents well the maximum dissipation rate in the rocky interior and the heat flux through the mantle surface (Figs. 6a,b,c,g,h,i in [8]). The dissipated power at the top of the mantle is a superposition of Patterns C and A, the former dominating for a homogeneous interior and the latter dominating if the core has a low density (Figs. 6d,e,f in [8]). Regarding the dissipation in the ice layer, Models 1/2/3 in [8] yield Patterns B/C/B at the bottom of the layer and Patterns A/C/A at the top of the layer (see their Fig. 10).

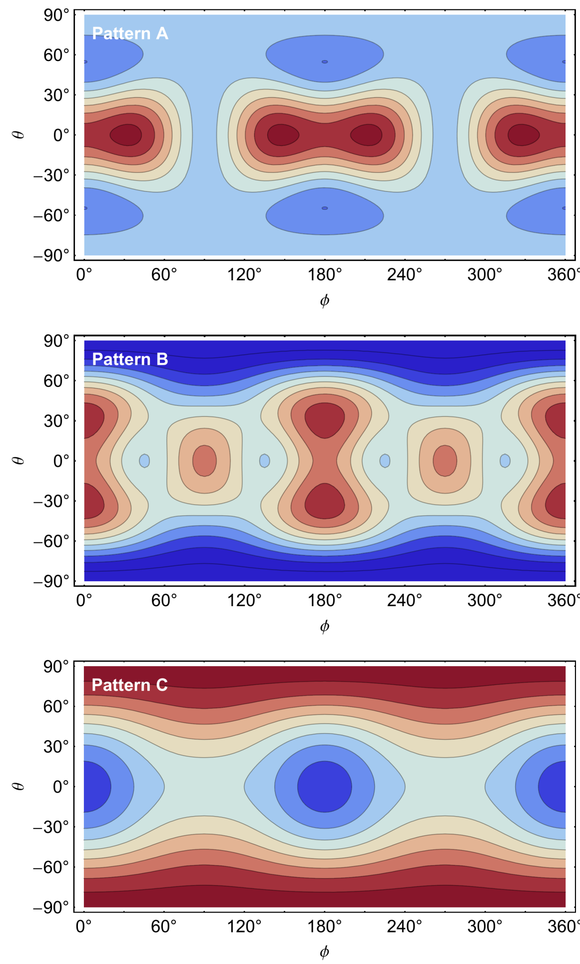

Figure 1: Spatial patterns of tidal heating of a body in synchronous rotation, given by Eqs. (4), each normalized by its RMS. Contours range from -2 (deep blue) to $+2$ (deep red) with an interval of 0.5.

References: [1] W. M. Kaula (1964) *Rev of Geophys* 2:661. [2] M. Segatz, et al. (1988) *Icarus* 75:187. [3] T. Spohn (1997) *Lecture Notes in Earth Sciences, Berlin Springer Verlag* 66:345. [4] G. W. Ojakangas, et al. (1989) *Icarus* 81:220. [5] M. Beuthe, et al. (2010) in *EPSC Abstracts Vol. 5* abstract EPSC2010-146. [6] B. G. Bills, et al. (2003) in *Lunar Planet. Sci. 34* abstract 1465. [7] S. J. Peale, et al. (1978) *Icarus* 36:245. [8] G. Tobie, et al. (2005) *Icarus* 177:534. [9] H. Takeuchi, et al. (1972) in *Methods in Computational Physics, vol. 1* (Edited by Bolt, B.A.) 217–295 Academic Press, New York.

Acknowledgements: This work was financially supported by the Belgian PRODEX program managed by the European Space Agency in collaboration with the Belgian Federal Science Policy Office.